Science in China Series D: Earth Sciences

www.scichina.com
earth.scichina.com
www.springerlink.com

Molecular fossil and paleovegetation records of paleosol S4 and adjacent loess layers in the Luochuan loess section, NW China

ZHANG HuCai[1,2], YANG MingSheng[1†], ZHANG WenXiang[1], LEI GuoLiang[1], CHANG FengQin[1], PU Yang[2] & FAN HongFang[1]

[1] Key Laboratory of Western China's Environmental Systems, Ministry of Education, College of Earth and Environment Sciences, Lanzhou University, Lanzhou 730000, China;
[2] State Key Laboratory of Lake and Environment Sciences, Nanjing Institute of Geography and Limnology, Chinese Academy of Sciences, Nanjing 210008, China

Using gas chromatography-mass spectrometry (GC-MS) technique, a series of biomarkers were identified, including *n*-alkanes, *n*-alkane-2-ones, isoprenoid etc. from the loess-paleosol samples collected from the S4 and adjacent L5, L4 of the Luochuan loess section, Northwestern China. Based on these data, especially *n*-alkanes and high-resolution magnetic susceptibility and grain size data, the paleoenvironment and paleovegetation history during S4 was reconstructed. The CPI (Carbon Predominance Index) and correlation between *n*-alkanes and magnetic susceptibility and grain size data demonstrated that the molecular fossils in paleosol and loess layers can reflect the vegetation condition during the loess-paleosol formation, if the allochthonous organic inputs could be excluded reasonably. The ACL (average chain length) index is correlated well with paleomagnetic susceptibility and grain size variations, displaying their good synchrony with warm and humid climate. However, it relatively lagged behind the paleomagnetic susceptibility and the grain size variations when the climate began to deteriorate. During the formation period of paleosol, the *n*-alkanes was dominated by C_{31} homologue, indicating that the primary organic input originated from herbs. Our study also demonstrated that the herbs were more flourish than wood plants in Loess Plateau, especially in the Luochuan area during the warm and humid phase, and there was no typical forest vegetation developed in the studied period.

paleoenvironment Paleosol S4, Luochuan loess section, biomarker, paleovegetation

Biomarker is a compound that could indicate the biologic origin of organic matters. Once the molecular structure and isotopic composition are identified, the source of the biomarkers and their composition character and distribution pattern could be figured out even to species level. Therefore, molecular fossil has been widely applied in the studies on paleoenvironmental and paleoclimatic changes[1,2], such as aerosol[3], marine sediment[4−6], lacustrine and peat sediment[7−10], stalagmite[11], snow and ice[12], loess-paleosol[13−15] and paleovegetation changes[16]. These works demonstrated the reliability of the biomarker research in the paleoclimate, paleoenvironment and paleovegetation and it could play an important role in tracking the environmental variation at molecular level.

The loess is widely distributed in the Northwestern China and has served as one of the best archives for paleoenvironment reconstruction. Together with deep sea sediments and ice core studies, they were considered mainstays of the global changes[17] and great achievements have been documented in the recent decades[18−22].

Received July 23, 2007; accepted October 30, 2007
doi: 10.1007/s11430-008-0012-9
†Corresponding author (email: yangmsh05@st.lzu.cn)
Supported by the Hundred Talent Project of Chinese Academy of Sciences and the National Natural Science Foundation of China (Grant No. 40371117)

However, as loess is one kind of aeolian accumulations, it is difficult to reconstruct paleovegetation change history because not only the sources of pollen are complex, but also its content is very low. Consequently, the paleovegetation condition during the loess-paleosol formation is scarce and there are few high-resolution researches in this aspect, especially on century-millennium scale.

Xie et al.[13] and Wang et al.[14] applied molecular biological method to discuss the paleovegetation evolution since the last glaciation in Loess Plateau. They suggested that the source of the molecular fossils in the loess included autochthonous and allochthonous origins. Zhang et al.[23,24] and Liu et al.[25] analyzed the expansion characteristics of the C3 and C4 vegetation types in the Luochuan loess section from the last glacial period, their results showed that the specific carbon isotopes could be treated as useful environmental variation proxies.

Theoretically, paleosol S4 in the loess-paleosol sequence corresponds to the Marine Isotope Stage 11 (MIS11) and was considered as an analogue climate model of Holocene and present. Therefore, investigation of the paleoenvironment and paleovegetation history during S4 is of crucial importance to understanding the mechanism of the climate changes in the context of global warming scenario and projection of the future climate. In this paper, we focus on the molecular fossils of S4 in Luochuan loess section, one of the typical loess sections in Northwestern China in reconstructing the paleovegetation and paleoenvironment history.

1 Sampling and methods

1.1 Study area and sampling

Luochuan loess section is located at the central part of the Chinese Loess Plateau under typical semi-arid—semi-humid climate. The average temperature of January and July is –6.4—–5 and 21.6—22.8℃, respectively, with an average annual temperature of 8—9℃. The annual precipitation is 550—630 mm and is mainly concentrated in the summer season (60%). The dominant vegetation is herbs, with locally developed secondary shrubs.

The samples were collected from a manually cleaned fresh cliff in the paleosol horizon of S4 together with parts of underlying L5 and overlaying L4 layers. It was sampled with 2 cm interval for paleomagnetic susceptibility and grain size analyses. A total of 55 samples were prepared for molecular fossil tests with samples from lower part of L4 and upper S4 taken in 4 cm interval, and those from the lower part of S4 and the upper part of L5 in 6 and 4 cm intervals respectively. All the samples were sealed and preserved in dry condition to avoid contamination and microbial decay.

1.2 Experimental analysis

After grinding to 178 μm, about 50 g samples for lipid analysis were ultrasonic-extracted with dichloromethane and methanol in volume ratio of 93∶7 for twice, with 20 min each time. The extracted material was then condensed and weighed. As the extracted material was only 4—12 mg in amount, it was not separated to family components using a silica gel-alumina chromatographic column, in order to prevent the loss of such components as micro-saturated hydrocarbon and oxygen compounds. After air-drying and diluting using chloroform, the samples were analyzed directly and immediately using GC-MS analysis.

As the organic matter content is often low in loess-paleosol samples, the organic contamination might affect the analysis result strongly. Therefore, all the reagent and filter paper used in the experiment were refined and distilled and all glass containers were washed using distilled water and soaked in the reagent for 5 min each time.

The GC-MS analysis was performed with using an HP 5973MSD interfaced to an HP6890 gas chromatograph fitted with a 30 m×0.25 mm i.d., fused silica capillary column, coated with a film (0.25 μm) of 5% phenyl-methyl-DB-5. For routine GC analysis, the temperature of the oven was heated from 80 to 300℃ at 3℃/min rate with the initial and final hold time of 1 and 30 min, respectively. Helium was used as carrier gas at a linear velocity of 32 cm/s, with the injector operating at a constant flow of 0.9 mL/min. The MS operated with an ionization energy of 70 eV, a source temperature of 230℃ and an electron multiplier voltage of 1900 V over the range of 35—550 Dalton. In order to identify the possible organic contaminations during the experimental processes we add a blank sample for reference and no organic composition discussed in this study was observed. Magnetic susceptibility was performed with using MS2 kappameter (Bartington) for three times for cross-validation and then average values were calculated.

Grain size analysis was conducted using MARVERN MS-2000 after following standard pre-processing procedures. All the experimental processes were verified by precision and reliability test strictly[26].

2 Results and discussions

2.1 Characteristics of the molecular fossil

A large amount of molecular fossils was identified in this study (Figure 1(a)). The carbon distribution of n-alkanes ranged from C_{15} to C_{34}, and showed a bimodal distribution pattern with weak peaking between C_{15} and C_{23} and major peaks occurring from C_{23} to C_{33}. The carbon number smaller than 23 showed an even-predominant but not conspicuous and the main peak carbon more than 23 possesses an odd-predominant maximizing at C_{31} (Figure 1(b)). The CPI (Carbon Predominance Index = $[(C_{25}+C_{27}+\cdots+C_{33})/(C_{24}+C_{26}+\cdots+C_{32}) + (C_{25}+C_{27}+\cdots+C_{33})/(C_{26}+C_{28}+\cdots+C_{34})]/2$) ranged from 1.87 to 4.38, smaller than that of plant wax in general, but larger than that of the high degree maturity organic matters. It demonstrated that the molecular fossil in Luochuan loess section was characterized of the organic matter with low maturity.

Theoretically, the distribution patterns of the molecular fossils demonstrate the origin of organic matters in the samples. Weak or even zero level of low carbon number molecular homologues implies limited contribution by microbial, algae and bacteria. The dominance by the high carbon number molecular indicates the higher plant contribution to the organic matter in samples.

2.2 Origin of organic matters

Loess is accumulated in a very different way from many typical types of sediment, such as lake and fluvial deposits. The source of loess is extremely complex not only because of its aeolian transportation and a broad geographical range of source area, but also due to a strong secondary and/or reworking processes and highly mixing property during sedimentation. In order to get reliable molecular fossil signals from the organic matter in the loess-paleosol layers, the *in situ* originated organic compounds should be separated from those transported from the source area. Using the property of CPI value of *n*-alkanes in geological dust and petroleum residue amount to 1, the contribution of the molecular fossils originated from high plants can be distinguished[12,27−29], using the equation: $C_{w/n}=C_n-[0.5(C_{n-1}+C_{n+1})]$, where $C_{w/n}$ is the autochthonous molecular fossils originating from the high plants. The negative value was settled to zero and C_n, C_{n-1} and C_{n+1} are homologous compounds in samples, which represent the total abundance of geological sources and organism sources respectively. This approach has been successfully applied to paleovegetation and paleoclimate studies (e.g. in the snow and ice[12]), and to distinguishing the *n*-alkanes distribution

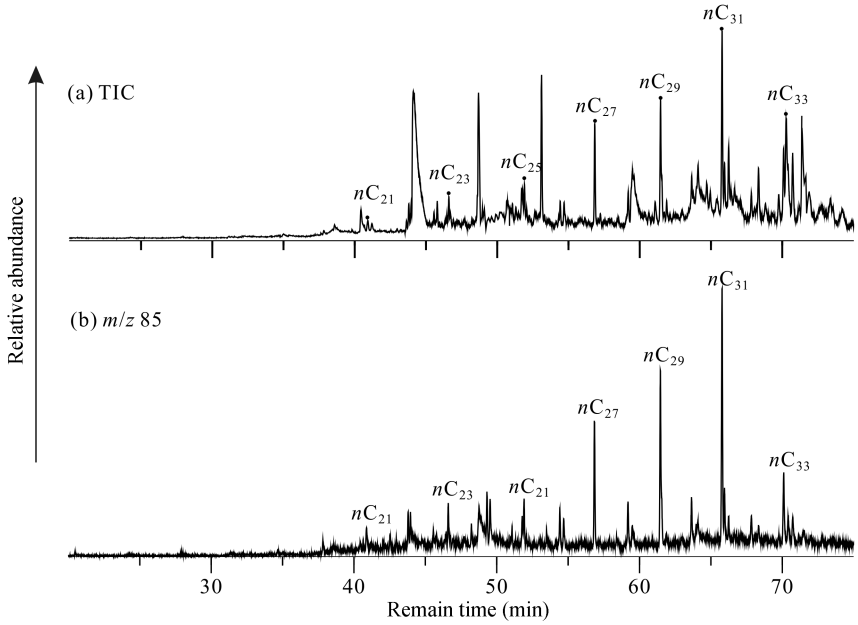

Figure 1 The GC-MS mass chromatograms of molecular fossils in S4, the number on each of the peaks is the carbon number. (a) Chromatogram for the total ions; (b) chromatogram for the *n*-alkanes.

of autochthonous and allochthonous origins in Jiuzhoutai loess section in Lanzhou[13].

The CPI values of the Luochuan loess samples were low, implying very low content of organic matter and a simple molecular fossil origination. It may also be due to a long time exposure in the open environment or the warm-humid climate, and to the strong pedogenetic processes during the S4 formation. Based on the formula mentioned above, the relative abundance of autochthonous *n*-alkanes in the samples from S4 and adjacent loess layers could be calculated. It was found that the high molecular weight homologues such as C_{29}, C_{31} and C_{33} mainly originated from autochthonous organic matters (mean values are 76%, 85% and 75%, respectively). But on the other hand, the low molecular weight homologues such as C_{23}, C_{25} and C_{27} were affected by allochthonous organic input (mean values are 19%, 33% and 56%, respectively) strongly, and possibly with the carbon number becoming smaller, the content of allochthonous originated *n*-alkanes increased. Because all the samples analyzed were dominate by C_{29}, C_{31} and C_{33} homologues and there was no sufficient amount of hopane identified in the samples, it was suggested that the allochthonous molecular fossil inputs were relatively low and therefore negligible. Another interesting phenomenon is that the relative ratios of allochthonous and autochthonous of C_{25} and C_{27} vary with both a high frequency and also a strong magnitude, the reasons are unknown and therefore, more studies are needed in the future.

Organic geochemical studies show that the *n*-alkanes originated from woods and grasses were preferentially dominated by C_{27} or C_{29} and C_{31} *n*-alkanes[30,31]. Therefore, it can be deduced that C_{31} homologues dominated samples imply that the main vegetation type was grassland, while the dominance by C_{27} and C_{29} homologues indicates the predominance of woody plants. That is to say, the C_{31}, C_{27} and C_{29} homologues can represent the relative biomass of woody and grass vegetations. The molecular fossil study on the modern forest vegetation and underneath soil from the semi-arid area of Xinglong Mountain near Lanzhou (Zhang et al., unpublished data) in west part of Loess Plateau showed that branches and leaf of deciduous broad-leaved trees were dominated by the C_{27} homologues and needle-leaved evergreen trees and leaves were dominate by C_{31} homologues. However, the molecular fossil of modern soils showed that C_{27}, C_{29} and C_{31} homologues all appeared in the samples even in the case that the soil had been developed under the forest, this posed a question that the molecular fossil of modern soils could be a mixture of all the vegetation types, and does not show clear differentiation of the vegetation coverage (Figure 6(a)). Relatively speaking, high molecular weight homologues of *n*-alkanes in Luochuan loess section was characterized of a simple distribution, maximizing at C_{31} or C_{29}, and was different from those in the modern soils (e.g. at Xinglong Mountain). This indicated sparse vegetation coverage with weak micro-organic processes, and also poor preservation condition for organic matters. For further comparisons, we use $Q_{\text{grass/plant}}$ ($q_{\text{grass/plant}}$)=$C_{31}/[C_{27} + C_{29} + C_{31}]$ and $Q_{\text{wood/plant}}$ ($q_{\text{wood/plant}}$)=$[C_{27}+C_{29}]/[C_{27}+C_{29}+C_{31}]$, to represent relative molecular fossil abundance of grass and woody plants in the loess-paleosol samples respectively. The index $Q_{\text{grass/plant}}$ represents the autochthonous molecular fossil between grass and woody plant; the index $q_{\text{grass/plant}}$ represents the uncorrected (including allochthonous) molecular fossil ratio between grass and woody plant.

Paleomagnetic susceptibility, which well matches the loess-paleosol cycles, is one of the best proxies for the Southeastern Asian summer monsoon[19,20]. Statistical analyses showed that there exists a high correlation between $Q_{\text{grass/plant}}$, $Q_{\text{wood/plant}}$ and paleomagnetic susceptibility (Figures 2(a) and (b)), with the correlation coefficients (r) of 0.783 and –0.739, respectively. Grain size variation in loess-paleosol sequence usually was used as an indicator for the winter monsoon strength. In the Luochuan loess section, it also showed a high correlation between $Q_{\text{grass/plant}}$, $Q_{\text{wood/plant}}$ and grain size with r values of –0.755 and 0.754, respectively (Figure 2(c) and (d)). All these pointed to that the autochthonous originated *n*-alkanes are representative of the vegetation development during the loess-paleosol formation.

Figure 3(a) and (b) show the correlations between uncorrected molecular fossil ratios of $q_{\text{grass/plant}}$, $q_{\text{wood/plant}}$ and paleomagnetic susceptibility (r=0.570 and –0.578, respectively) and all could pass the significant test at p-level of 0.01 and 0.05. Similarly, strong correlations between $q_{\text{grass/plant}}$, $q_{\text{wood/plant}}$ and the medium grain size are shown in Figure 3(c) and (d) (r = 0.703 and –0.702, respectively), indicating a high correlation between them. Noticeably the correlation between $Q_{\text{wood/plant}}$ and paleomagnetic susceptibility (r=–0.739) was higher than that between $q_{\text{wood/plant}}$ and magnetic susceptibility (r =

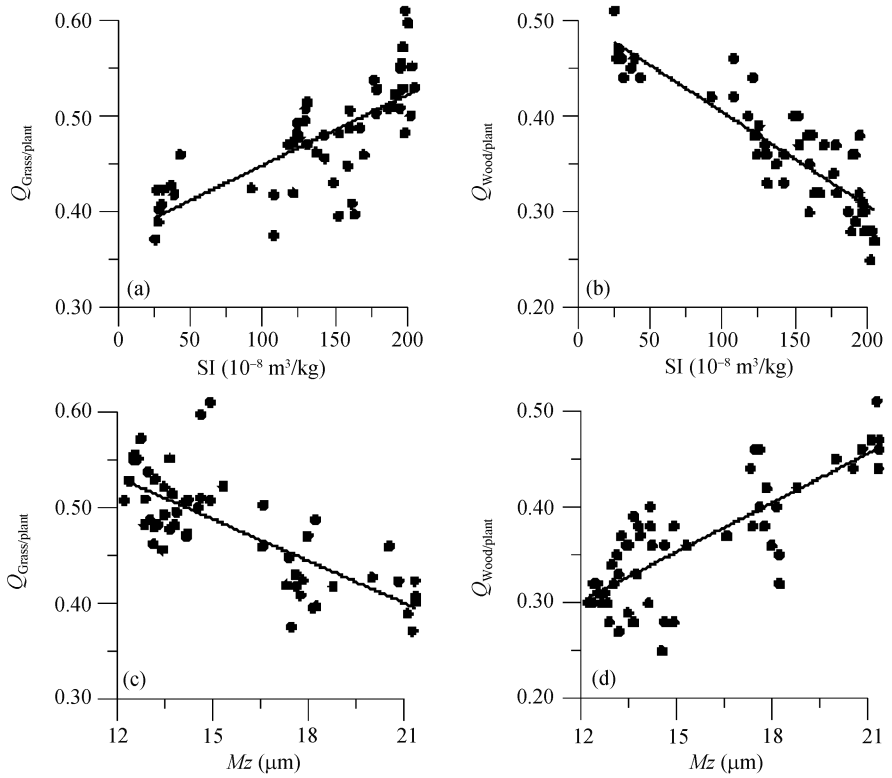

Figure 2 Correlation between autochthonous molecular fossils between susceptibility and the grainsize.

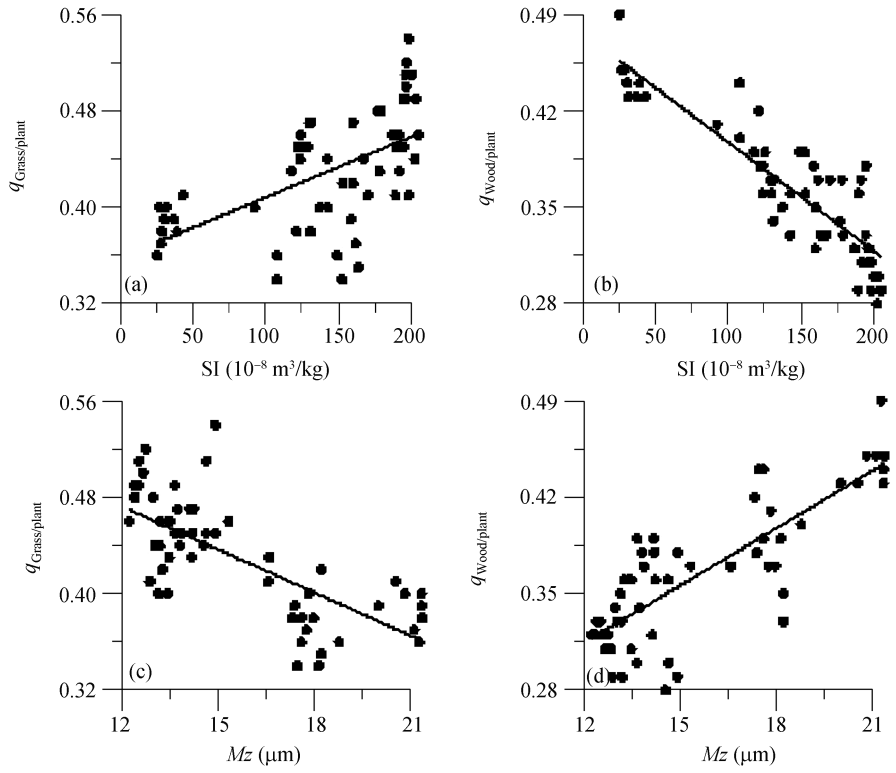

Figure 3 The correlation between uncorrected molecular fossils and susceptibility, grainsize.

–0.578). The correlation between $Q_{grass/plant}$ and susceptibility (r=0.783) was significantly higher than that between $q_{grass/plant}$ and susceptibility (r = 0.570). As shown in Figure 3 the correlation of $q_{grass/plant}$ or $q_{wood/plant}$ with the paleomagnetic susceptibility is much weaker than that between $Q_{grass/plant}$ or $Q_{wood/plant}$ to the paleomagnetic susceptibility. This indicated that the corrected molecular fossils can represent autochthonous vegetations as the organic matter source, which can adapt to the local climate and landscapes. This result is in consistence with the fact that there is little vegetation coverage in Gobi desert areas, which was considered as a main source of the dust materials. Zhang et al.[24] showed that the majority of lipid in Loess Plateau had autochthonous sources. A stronger correlation between $Q_{grass/plant}$ and paleomagnetic susceptibility (r=0.783) than that between $q_{grass/plant}$ and paleomagnetic susceptibility (r=0.570) probably indicated that the organic compositions originating from herbs are vulnerable to the influence of allochthonous source, due to the vegetation dominance by grasses in loess areas.

2.3 Average chain length (ACL) and paleoenvironment

The wax *n*-alkanes from higher plants could be well preserved in sediments. Earlier studies showed that the n-alkanes of different plants have different chain lengths. Therefore, the average carbon chain length values (ACL=C_{27}—C_{33} averaged chain length) could represent different vegetation types[32] and the ACL value might reflect the local temperature variation[33]. In the subtropical area the leaf wax of terrestrial plants produces longer carbon chain compounds. In comparison carbon chain compounds are often shorter in temperate area. The carbon chain length of *n*-alkanes could be well preserved in warmer rather than colder area[34]. Because the humidity can affect physiological functioning of plants, as well as the photosynthesis and material synthesis process, the average length of the carbon chain is strongly associated with humidity of the environment[35]. It has been shown that the average length of the *n*-alkanes in peat reflected the relative temperature and humidity conditions in the region[36].

In the transition phase from L5 to S4, paleomagnetic susceptibility and grain size variations suggest that (Figure 4) the winter monsoon weakened gradually and the climate shifted from cold-dry to the warm-wet. In this case the average length of carbon chain becomes shorter. During the paleosol formation under a warm-humid climate condition, the strength of summer monsoon in the study area intensified gradually. With the sediments shifting from S4 to L4, paleomagnetic susceptibility weakened significantly in contrast to weaker variation of ACL values, indicating that the ecosystem was relatively stable even when the climate deteriorated. The trend of ACL variation was consistent with the changing of the local climate during the period from the cold-dry stage to the warm-humid one, or from the loess accumulation phase to the paleosol formation one. However, there were some deviations from these, e.g. the ACL records generally lagged behind during such a transition. During the last 170 ka, the ACL data of the

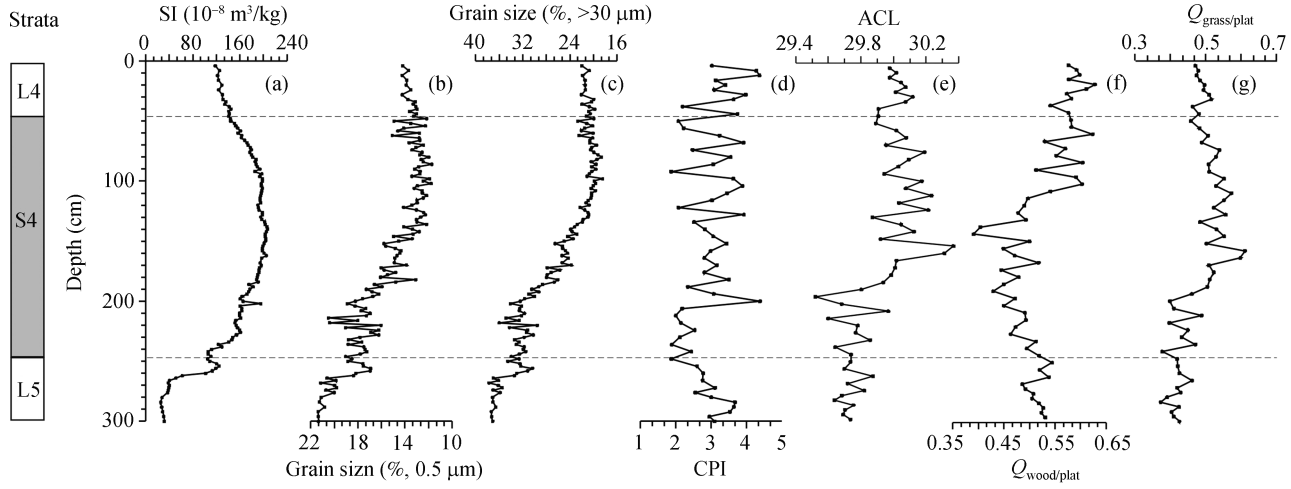

Figure 4 The paleomagnetic susceptibility, grainsize and the ratio of *n*-alkanes. S_4 is paleosol, L_5 and L_4 are loess, $Q_{wood/plant}$ = $C_{29}/(C_{27}+C_{29}+C_{31})$, $Q_{grass/plant}$ =$C_{31}/(C_{27}+C_{29}+C_{31})$, ACL=$\sum(C_n\times[C_n])/\sum[C_n]$, $[C_n]$ is the relative abundance of the *n*-alkanes, *n* is the carbon number of the *n*-alkanes, *n* range from 25 to 33.

Luochuan loess-paleosol profile was low in the L2 section, increased gradually at the L2/S1 transitional stage, but was high in the paleosol S1[24].

2.4 Vegetation reconstruction of the paleosol S4

The abundance of *n*-alkanes and related parameters showed that C_{31} and C_{29} homologues were the dominated n-alkanes in all samples. The carbon distributions in the depth from 300 to 230 cm (sample L5-7-1) peaked at C_{29} homologue. In the depth from 230 to 0 cm (sample S4-34-1 and L4-7-1) with peak at C_{31} homologue and in samples L5-4 and L5-5, the abundances of C_{29} and C_{31} are equal. It is noteworthy that the carbon number maximums vary in some samples from S4, showing that the vegetation was not always dominated by grass under a warm humid climate condition, but changed along with the climate oscillations. The paleomagnetic susceptibility and grainsize indexes showed that in the transitional period from loess accumulation to paleosol formation, the carbon number maximum changed frequently.

The indexes of $Q_{\text{grass/plant}}$ and $Q_{\text{wood/plant}}$ represent the relative abundance of grass and woody vegetations. During the transitional process from L5 to S4, the value of $Q_{\text{grass/plant}}$ was smaller than that of $Q_{\text{wood/plant}}$, showing a higher proportion of woody plant than grass, indicating monotonous vegetation coverage under the relatively cold-dry climate and a low vegetation biomass. With the improvement of the climate and environment, the value of $Q_{\text{grass/plant}}$ increased gradually while $Q_{\text{wood/plant}}$ reduced gradually, implying that the vegetation changed from woody dominance to the grass one. During the period of S4 paleosol formation, the paleomagnetic susceptibility and grainsize data indicated that the summer monsoon strengthened, and the humidity and temperature increased significantly. The environment favored the vegetation production and diversification. However, in areas such as Chinese Loess Plateau, the hydrothermal phasing condition was more favorable to the grass growth, resulting in the blooming of the herbs during formation of S4, a warm humid period for pedogenesis. The value of $Q_{\text{grass/plant}}$ increased gradually until reaching the maximum. Meanwhile, the value of $Q_{\text{wood/plant}}$ decreased gradually due to the expanding of grass. During the transitional period from S4 to L4, paleomagnetic susceptibility decreased obviously, but the grainsize (mediam diameter portion and >30 μm portion) only showed small change. This phenomenon (with a signify-cant change of paleomagnetic susceptibility but a small grainsize changes) implied that when the climate deteriorated at the end of S4, weakening of the pedogenetic process was mostly resulted from a weakening of the summer monsoon. At that time, although the abundance of C_{29} homologue increased gradually, the C_{31} homologue was still the dominate compound even though the n-alkanes parameter of $Q_{\text{grass/plant}}$ decreased relatively. The increase of $Q_{\text{wood/plant}}$ indicated that the grass production decreased and woody plants flourished in the transition from the interglacial to glacial climate. This variation could be summed up as a vegetation type dominated by the grass in the warm and humid climate condition during that paleosol formed, but by woody plants during the cold and dry climate when loess accumulated. The molecular fossils in loess-paleosol sequence were determined by the total vegetation biomass, especially the portion of grass.

The relative abundance of *n*-alkanes was used to distinguish vegetation types, for example, Hanisch et al.[37] considered that the C_{27} and C_{29} homologues of *n*-alkanes originated from the deciduous trees, therefore, the ratio of $(C_{27}+C_{29})/\Sigma(C_{23}+\cdots+C_{33})$ was used to estimate the contribution of deciduous trees to the lacustrine sediments. Schwark et al.[38] used the ratio of C_{29}/C_{31} to indicate the relative abundance of tree and grass to reconstruct the vegetation variation from postglacial period to late Holocene. They believed that in central Europe, the *n*-alkanes ratio of $C_{31}/(C_{29}+C_{31})$ in sediment was larger than 0.5 during postglacial period, and smaller than 0.5 under forest coverage during the Holocene. Schefuss et al.[35] and Rommerskirchen et al.[39] used normalized $C_{31}/(C_{29}+C_{31})$ index of *n*-alkanes to discuss the vegetation variation of continental margin in South Africa mainland. They suggested that this index was relatively high in grassland or extensive grassland. The ratio of $C_{31}/(C_{29}+C_{31})$ in the drilling samples collected from offshore of South Africa mainland were larger than 0.5, implying a strong input of grasses. Lei et al.[26] conducted a similar study on Luochuan loess, concluded that the grass was the dominated vegetation since 170 ka BP, and found the $C_{31}/(C_{29}+C_{31})$ values ranged from 0.5 to 0.81, with a increased value in the warm stages but decreased one in cold and dry stages. It means that herbs increased in warm-humid period and decreased in cold-dry period. Here we used the same ratio to compare our data with that of others. Triangular diagram of

n-alkanes of S4 and the adjacent loess layers in Luochuan loess section as well as $C_{31}/(C_{29}+C_{31})$ ratio variations along the profile were shown in Figure 5. It showed that with the development of paleosol S4, the grass increased relatively. However, woody plants increased during the period of loess accumulation (Figure 5(a)), and the $C_{31}/(C_{29}+C_{31})$ values range from 0.45 to 0.85. In loess layer L5, the $C_{31}/(C_{29}+C_{31})$ values of L5-13-L5-6、L5-3 - L5-1 are smaller than 0.5 while that of L5-5 and L5-4, as well as the L4 and S4 are slightly larger than 0.5, only that of S4-29 is smaller than 0.5. Therefore, it can be deduced that sparse shrubs dominated the vegetation during L5, and was typical desert vegetation. Grass dominated the vegetation in S4 and adjacent L4, and was savanna vegetation. This is consistent with the pollen data in Luochuan S4 which showed the dominate vegetation might be forest grassland vegetation[18], even though the amount and component of pollen varied dramatically. At the same time, the pollen data from nearby Huangling loess profile indicated that the vegetation was dominated by grass during the time[40]. Stable isotope studies on Luochuan loess section showed that C3 plants dominated the vegetation during the loess deposits period but C4 plant expanded dramatically during the period of paleosol formation. Because the climate condition was much more harsh during loess accumulation than that of paleosol formation, the desert vegetation developed during the loess accumulation period when the climate was cold and dry[41], which is consistent with our results.

During the formation period of paleosol S4, leaching processes enhanced and the calcium nodule formed. This process may lead to molecular fossils migrating downwards. As the leaching effects roughly equal to the homologues carbons with a similar or almost similar numbers (such as *n*-alkanes C_{27}, C_{29} and C_{31} homologues), their ratios also should be similar. That is to say, even if the leaching effects could affect individual compounds of C_{27}, C_{29} and C_{31} homologues contents, they do not affect the ratio to reflect the variation of vegetation. In the illuvial (or B) horizon, *n*-alkanes distribution might be affected by leaching process. In the lower part of paleosol S4, C_{31} dominates but C_{29} dominates in the underneath loess (the upper part of L5), the leaching process might be weakening the dominance of the C_{29} in loess layer. Moreover, the leaching effect mainly occurs in dissolved state but dissolved organic matter content is very limited in the loess-paleosol. In the large-scale transformation such as loess-paleosol cycles, leaching effect does not influence the molecular fossil distribution patterns obviously, in which C_{31} homologue indicated grass vegetation dominated during the paleosol formation but C_{29} indicated woody plant domination during the loess accumulation.

3 Conclusions

Molecular fossils were abundant in loess-paleosol sequences of the Luochuan profile and recorded important but often neglected information for paleovegetation and paleoenvironment reconstruction. The ratios of *n*-al-

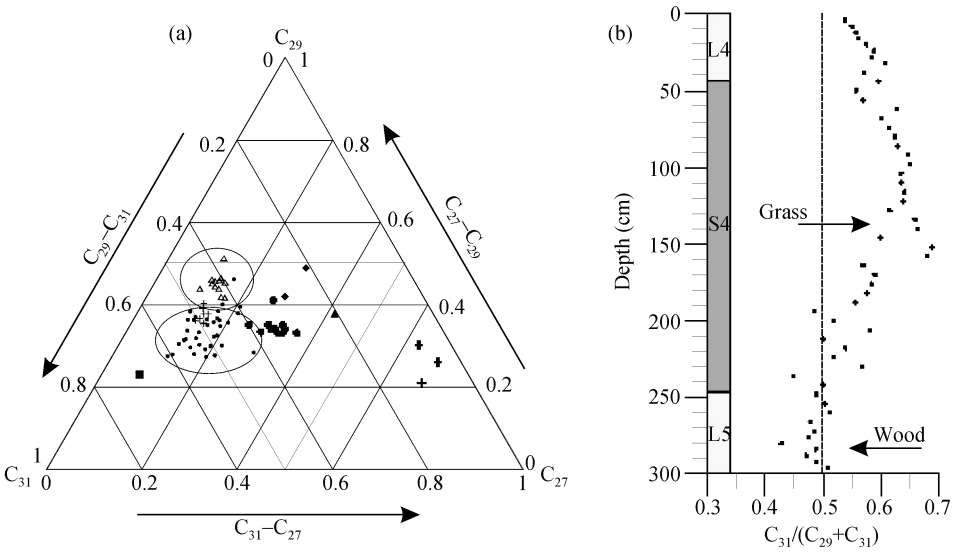

Figure 5 Triangular diagram of n-alkanes in Luochuan profile and the classification based on $C_{31}/(C_{29}+C_{31})$ parameters. (a) •, S4; +, L4; the Loess; Δ, L5 loess; ■, grass; ✹, soil; ♦, pine needles-fir leaves; ▲, moss; ✚, broad-leaved-branch-the trunk.

kanes, such as q_{grass}/q_{plant} and q_{wood}/q_{plant}, Q_{grass}/Q_{plant} and Q_{wood}/Q_{plant}, together with the grain size and susceptibility data, showed that molecular fossils in loess-paleosol were closely related to the environmental variations through the shift of vegetation types. Noticeably the correlation between q_{grass}/q_{plant} and paleomagnetic susceptibility was weaker than that between Q_{grass}/Q_{plant} and the susceptibility.

Based on the correlation between grain size and magnetic susceptibility, it was found that the ACL value, an important index of the temperature and humidity, was relatively higher in the paleosol, indicating a warm-humid climatic phase, and relative low in the loess possibly under a cold-dry climatic condition. The ACL value is related closely to the regional vegetation coverage. During the transition from cold-dry climate to warm-humid, ACL value changed synchronously. However, when it changed from a warm-humid to a cold-dry climate condition, the vegetation coverage density and species varied randomly. It seems that the vegetation community shows its insensitivity to the environment changes, resulting in an inactive ACL response.

The *n*-alkanes from S4 and adjacent loess L5, L4 layers in Luochuan loess section showed that woody plants decreased in the transitional process from L5 to S4, while the corresponding proportion of grass vegetation increased, indicating that the grass expanded when the climate changed from the cold and dry to warm and humid. The carbon number distribution of *n*-alkanes dominated by C_{29} homologue in loess layer indicated preferential woody input during the loess accumulation, corresponding to an increased winter monsoon and weakening of the summer monsoon. During the soil development period, the *n*-alkanes with maxima at C_{31} homologue showed the dominance of grass vegetation. During the transition from S4 to L4, even though the samples were still dominated by the C_{31} homologue, the C_{29} homologue showed an increasing tendency. Such variation is consistent with the loess-paleosol change rhythm. As an index of vegetation types, $C_{31}/(C_{29}+C_{31})$ ratio shows that the dominate vegetation is woody plant in loess and is grass vegetation in paleosol. This phenomenon reveals that the vegetation types were controlled by the temperature and precipitation changes.

Molecular fossil is one of the most useful proxies for reconstruction of paleovegetation and environment in loess-paleosol sequence. It provides a new geochemical method to tackle the paleoenvironmental problems on molecular level though there are many open questions waiting for further investigations.

Special thanks to two anonymous reviewers for their constructive comments that improved the manuscript greatly.

1 Fu J M, Sheng G Y. Molecular organic geochemistry and its application to the study of paleoclimate and paleoenvironments. Quat Sci (in Chinese with English abstract), 1992, (4): 306－320

2 Ohkouchi N, Kawamura K, Taira A. Molecular paleoclimatology: Reconstruction of climate variabilities in the late Quaternary. Org Geochem, 1997, 27: 173－183

3 Simoneit B R T, Sheng G Y, Chen X J, et al. Molecular marker study of extractable organic matter in aerosols from urban areas of China. Atmos Environ, 1991, 25A(10): 2111－2129

4 Volkmam J K, Barrett S M, Blackbum S I, et al. Allkenones in gephyrocapsa oceanica: Implications for studies of paleoclimate. Geochim Cosmochim Acta, 1995, 59: 513－520

5 Pearson A, McNichol A P, Benitez-Nelson B C, et al. Origins of lipid biomarkers in Santa Monica Basin surface sediment: A case study using compound——Specific $\Delta^{14}C$ analysis. Geochim Cosmochim Acta, 2001, 65: 3123－3137

6 Lu B, Chen R H, Wang Z P, et al. Ocean environment change in the Bering Sea over the past 100 years——Evidences from the molecular fossil. Sci China Ser D-Earth Sci, 2005, 48(4): 555－564

7 Meyers P A, Ishiwatari R. Lacustrine Organic Geochemistry: An overview of indicators of organic matters sources and diagenesis in lake sediments. Org Geochem, 1993, 20(7): 867－900

8 Zhang H C, Chang F Q, Li B, et al. Branched aliphatic alkanes of the Late Pleistocene paleolake deposits from the Qaidam Basin, NE Tibetan Plateau. Chin Sci Bull, 2007, 52(9): 1248－1256

9 Sheng G Y, Cai K Q, Yang X X, et al. Long-chain alkenones in Hotong Qagan Nur lake sediments and its paleoclimatic implications. Chin Sci Bull, 1999, 44(3): 259－263

10 Xie S C, Evershed R P. Peat molecular fossils recording climatic variation and organism replacement. Chin Sci Bull, 2001, 46(10): 863－866

11 Xie S C, Yi Y, Huang J H, et al. Lipid distribution in a subtropical southern China stalagmite as a record of soil ecosystem response to paleoclimate change. Quat Res, 2003, 60(3): 340－347

12 Xie S C, Yao T D, Kang S C, et al. Geochemical analysis of a Himalayan snowpit profile: Implication for atmospheric pollution and climate. Org Geochem, 2000, 31: 15－23

13 Xie S C, Wang Z Y, Wang H M, et al. The occurrence of a grassy vegetation over the Chinese Loess Plateau since the last inter-glacier: The molecular fossil record. Sci China Ser D-Earth Sci, 2002, 45(1): 53－62

14 Wang Z Y, Xie S C, Chen F H. *n*-Alkane distributions as indicators for paleo-vegetation from Yuanbao S1 paleosol in Linxia, Gansu Province. Quat Sci (in Chinese with English abstract), 2004, 24 (2):

231－235
15 Yang M S, Zhang H C, Lei G L, et al. Biomarkers in weakly developed paleosol (L1SS1) in the luochuan loess section and reconstructed paleovegetation-environment during the interstade of the last glaciation. Quat Sci (in Chinese with English abstract), 2006, 26(6): 984－996
16 Mitra S, Bianch T S, Guo L, et al. Terrestrially derived dissolved organic matter in the Chesapeake Bay and the Middle Atlantic Bight. Geochim Cosmochim Acta, 2000, 64: 3547－3557
17 Williams M A J, Dunkertey D L, de Deckker P, et al. Quaternary Environments. Beijing: Science Press, 1997. 189－239
18 Liu T S. Loess and the Environment. Beijing: China Ocean Press, 1985. 1－251
19 Kukla G J, Heller F, Liu X M, et al. Pleistocene climate in China dated by magnetic susceptibility. Geology, 1998, 16: 811－814
20 An Z S, Porter S, Kukla G, et al. The susceptibility evidence of the monsoon variation in the Loess Plateau since recent 130,000 years. Chin Sci Bull, 1990, 35(7): 529－532
21 Yang M S, Zhang H C, Ding H, et al. ^{14}C dating of paleosol and animal remains in loess deposit: A comparative study. Earth Sci-J China Univ of Geosci (in Chinese with English abstract), 2005, 30(5): 589－596
22 Kukla G, An Z. Loess stratigraphy in central China. Palaeogeogr Palaeoclimatol Palaeoecol, 1989, 72: 203－225
23 Zhang Z H, Zhao M X, Lu H Y, et al. Lower temperature as the main cause of C4 plant declines during the glacial periods on the Chinese Loess Plateau. Earth Planet Sci Lett, 2003, 214: 467－481
24 Zhang Z H, Zhao M X, Eglinton G, et al. Leaf wax lipids as paleovegetational and paleoenvironmental proxies for the Chinese Loess Plateau over the last 170 kyr. Quat Sci Rev, 2006, 25: 575－594
25 Liu W G, Huang Y S, An Z S, et al. Summer monsoon intensity controls C4/C3 plant abundance during the last 35 ka in the Chinese Loess Plateau: Carbon isotope evidence from bulk organic matter and individual leaf waxes. Palaeogeogr Palaeoclimatol Palaeoecol, 2005, 220: 243－254
26 Lei G L, Zhang H C, Zhang W X, et al. The reliability and significance of the grainsize obtained by Mastersize 2000 laser analyzer. Acta Sediment Sin (in Chinese with English abstract), 2006, 24(4): 531－539
27 Simoneit B R T, Cardoso J N, Robinson N. An assessment of terrestrial higher molecular weight lipid compounds in aerosol particulate matter over the south Atlantic from about 30－705. Chemosphere, 1991, 23: 447－465
28 Sicre M A, Marty J C, Saliot A, et al. Aliphatic and aromatic hydrocarbons in different sized aerosols over the Mediterranean Sea: Occurrence and origin. Atmos Environ, 1987, 21(10): 2247－2259
29 Schneider J K, Gagosian R B, Cochran J K, et al. Particle size distribution of *n*-alkanes and ^{210}Pb in aerosols off the coast of Peru. Nature, 1983, 304: 429－432
30 Cranwell P A. Chain-length distribution of *n*-alkanes from lake sediments in relation to post —— Glacial environmental change. Freshwater Biol, 1973, 3: 259－265
31 Cranwell P A, Eblinton G, Robinson N. Lipids of aquatic organisms as potential contributors to lacustrine sediments. Org Geochem, 1987, 11: 513－527
32 Schwark L, Zink K, Lechterbeck J. Reconstruction of postglacial to early Holocene vegetation history in terrestrial Central Europe via cuticular lipid biomarkers and pollen records from lake sediments. Geology, 2002, 30: 463－466
33 Poynter J G, Farrimond P, Brassel S C, et al. Aeolian-derived higher-plant lipids in the marine sedimentary record: Links with paleoclimate. In: Leinen M, Sarnthein M, eds. Palaeoclimatology and Palaeometeorology: Modern and Past Patterns of Global Atmosphere Transport. Amsterdam: Kluwer, 1989. 426－435
34 Zhou W J, Xie S C, Meyers P A, et al. Reconstruction of late glacial and Holocene climate evolution in southern China from geolipids and pollen in the Dingnan peat sequence. Org Geochem, 2005, 36: 1272－1284
35 Schefuss E, Ratmeyer V, Stuut J B W, et al. Carbon isotope analysis of *n*-alkanes in dust from the lower atmosphere over the central eastern Atlantic. Geochem Cosmochim Acta, 2003, 67 (10): 1757－1767
36 Gagosian R B, Peltzer E T, Merrill J T. The importance of atmospheric input of terrestrial organic material to deep sea sediments. Org Geochem, 1986, 10: 661－669
37 Hanisch S, Ariztegui D, Püttmann W. The biomarker record of Lake Albano, central Italy —— Implications for Holocene aquatic system response to environmental change. Org Geochem, 2003, 34: 1223－1235
38 Schwark L, Zink K, Lechterbeck J. Reconstruction of Postglacial to Early Holocene vegetation history in terrestrial Mid-Europe via cuticular lipid biomarkers and pollen records from lake sediments. Geology, 2002, 30: 463－466
39 Rommerskirchen F, Eglinton G, Dupont L, et al. A north to south transect of Holocene southeast Atlantic continental margin sediments: Relationship between aerosol transport and compound-specific δ^{13}C land plant biomarker and pollen records. Geochem Geophys Geosys, 2003, 4(12): 1101
40 Shi J S, Li Z H, Wei M J, et al. Loess and Paleoclimate Evolution (in Chinese). Beijing: Geological Press, 1998. 26－34
41 Fakes L A, Sun J A. Carbon isotope record of the upper Chinese loess sequence estimates of plant types during stadials and interstadials. Palaeogeogr Palaeoclimatol Palaeocol, 1994, 108: 183－189